Langmuir

Article

pubs.acs.org/Langmuir

Molecular Thermodynamic Modeling of Droplet-Type Microemulsions

Livia A. Moreira and Abbas Firoozabadi*

Department of Chemical and Environmental Engineering, Mason Laboratory, Yale University, New Haven, Connecticut 06520-8286, United States

ABSTRACT: Microemulsions are nanoheterogeneous, thermodynamically stable, spontaneously forming mixtures of oil and water by means of surfactants, with or without cosurfactants. The pledge to use small volumes of amphiphile molecules compared to large amounts of bulk phase modifiers in a variety of chemical and industrial processes, from enhanced oil recovery to biotechnology, fosters continuous investigation and an improved understanding of these systems. In this work, we develop a molecular thermodynamic theory for droplet-type microemulsions, both water-in-oil and oil-in-water, and provide the theoretical formulation for three-component microemulsions. Our thermodynamic model, which is based on a direct minimization of the Gibbs free energy of the total system, predicts the structural and compositional features of microemulsions. The predictions are compared with experimental data for droplet size in water−alkane−didodecyl dimethylammonium bromide systems.

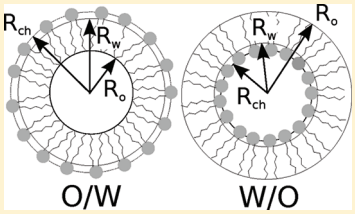

INTRODUCTION

In the last few decades, there has been increasing interest in microemulsions primarily because of their scientific importance and technological potential.[1] Microemulsions are thermodynamically stable dispersions of oil and water stabilized by a surfactant and, in many cases, also a cosurfactant.[2] The addition of amphiphilic surfactant to oil and water causes the separation of the oil-rich domain from the water-rich domain by the spontaneous assembly of the surfactants at the interface of the immiscible water and oil phases. Droplet-type and bicontinuous microemulsions are typical examples among the structured liquid phases. The droplet-type microemulsions can be spherical oil droplets dispersed in a continuous medium of water (oil-in-water microemulsions, O/W) or spherical water droplets dispersed in a continuous medium of oil (water-in-oil microemulsions, W/O). The O/W and W/O can be either a single-phase system or part of a two-phase system wherein the microemulsion phase coexists with an excess phase (an upper phase of excess oil in the case of O/W and a lower phase of excess water in the case of W/O). There are also nondroplet-type microemulsions, referred to as bicontinuous or middle-phase microemulsions. In this case, the microemulsion phase may be part of a three-phase system with the microemulsion phase in the middle coexisting with an upper phase of excess oil and a lower phase of excess water.[3]

One of the main goals of this work is to provide a general framework that allows the prediction of the phase behavior of different microemulsion types based on a global minimization of the total Gibbs free energy. The equality of the chemical potentials often used in the literature may not provide correct results, especially for such a complex system. Toward this purpose, we first write the expression for the total Gibbs free energy and then minimize the total Gibbs free energy for a system with a given overall composition, temperature, and pressure with respect to the geometrically and compositionally independent variables.

Different approaches have been used to describe the thermodynamics of microemulsions. The first efforts in the thermodynamic modeling of microemulsions relied on conventional liquid−liquid equilibrium by using a simple expression of the excess Gibbs energy derived from the Flory theory.[4−6] The main limitation of this type of modeling is the requirement of adjustable parameters from experimental data regression.

Another line of research allocates efforts to developing a thermodynamic understanding of microemulsions following the phenomenological theories of globular microemulsions.[7−12] In this work, the microemulsion systems are examined under a macroscopic thermodynamics point of view. The free energy of the droplet microemulsions is formulated from the known or estimated interfacial tension and bending free energy of the monolayer. One limitation of this type of model is that it cannot provide detailed properties of the phases and global phase behavior.[13]

A molecular theory of microemulsions has been proposed by Nagarajan and Ruckenstein.[3] This approach differs from the phenomenological thermodynamics formulation by looking at the molecular level for the surfactant self-assembly. This is the main molecular thermodynamic model in the literature. To the best of our knowledge, Nagarajan and Ruckenstein's formulation has not been compared against experimental data.

In this work, we present a predictive molecular thermodynamic model to droplet-type microemulsions. First, we derive the expression for the total Gibbs free energy for W/O and O/W droplet-type microemulsions. We include the excess phase in our derivations for the Gibbs free energy of droplet-type microemulsions, so the formulations account for both single-phase and two-phase systems. The Gibbs free energy minimization defines the existence of the excess phase and its size and composition as well as the size and composition of the continuous phase and droplets.

Received: October 5, 2011
Revised: December 6, 2011
Published: December 8, 2011

The expression for the total Gibbs free energy is used together with the free energy of aggregation in order to calculate the Gibbs free energy of the microemulsion. In the free energy of aggregation, we account for various contributions related to the headgroups and the interfacial layer. For a given overall composition, temperature, and pressure, we minimize the total Gibbs free energy in order to predict the compositional and geometrical features of the microemulsion. We believe that using the overall composition as a control variable is convenient because it allows for a direct comparison with the experimental data. The minimization is performed with respect to eight independent variables. We verify the model by comparing the predictions with experimental data for a three-component ionic microemulsion: didodecyl dimethylammonium bromide/water/alkanes.[14]

In this work, our derivations are limited to three-component microemulsions. Three-component ionic microemulsions have considerable advantages over conventional four- or five-component microemulsions in the field of elucidation of the microstructure. Surfactants such as didodecyl dimethylammonium bromide (DDABr) and dioctyl sodium sulfosuccinate (AOT) are known to form three-component ionic microemulsions and have been extensively investigated in studies on microemulsions characterization.[14−23] In the future, we will extend our formulations to include cosurfactants and electrolytes in the model. We will also expand our work to include bicontinuous microemulsions.

MOLECULAR THERMODYNAMIC MODEL

Our goal is to predict the phase behavior of microemulsions by minimizing the total Gibbs free energy. Toward this objective, we investigate the droplet-type microemulsions. In our formulation, we include the excess phase so that the Gibbs free energy minimization determines if the system is single-phase or two-phase. In the following section, we derive the expression for the total Gibbs free energy for W/O and O/W droplet-type microemulsions, which can be minimized with respect to geometrically and compositionally independent variables for a given overall composition, temperature, and pressure. We provide a brief description and the expressions for major contributions to the free energy of aggregation. We present the models used to describe the nonidealities of the solution related to the hard-sphere interactions due to the presence of droplets and to the mutual solubilities of the ternary system. We discuss the geometrical and compositional aspects and constrains for the minimization of the total Gibbs free energy.

Water-in-Oil Droplet Microemulsions. Consider a microemulsion system is composed of N_O oil molecules, N_S surfactant molecules, and N_W water molecules at temperature T and pressure p. The water-in-oil microemulsion has a continuous oil phase and a lower phase of excess water as schematically represented in Figure 1.

The continuous oil phase is composed of N_O^O oil molecules, N_S^O surfactant molecules, N_W^O water molecules, and N_g droplets. The subscript refers to the type of species, and the superscript refers to the phase. Each droplet is composed of g_O oil molecules, g_S surfactant molecules, and g_W water molecules. g for a droplet denotes the total number of molecules of different kinds present in it (i.e., $g = g_O + g_S + g_W$). We assume that the average properties of the continuous phase that contains the droplets are strongly influenced by the species present in the largest number and use the maximum term approximation.[3]

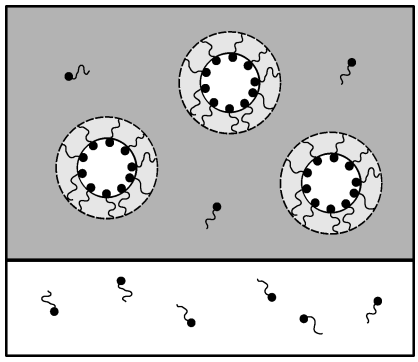

Figure 1. Schematic representation of a two-phase water-in-oil droplet microemulsion.

The interfacial layer of the droplet is composed of g_O^I oil molecules and g_S^I surfactant molecules, which gives a total of N_O^I oil molecules and N_S^I surfactant molecules forming the interfacial droplet layer:

$$N_O^I = g_O^I N_g \tag{1a}$$

$$N_S^I = g_S^I N_g \tag{1b}$$

The interfacial layer is a hydrophobic region that excludes the headgroups of the surfactant molecules and is assumed to be free of water molecules ($g_W^I = 0$ and $N_W^I = 0$). The aqueous core of the disperse droplets is composed of g_O^{core} oil molecules, g_S^{core} surfactant molecules, and g_W^{core} water molecules. The excess water phase is composed of N_O^{ex} oil molecules, N_S^{ex} surfactant molecules, and N_W^{ex} water molecules summing to a total of N_O^W, N_S^W, and N_W^W oil, surfactant, and water molecules, respectively, in the water phases.

$$N_O^W = N_O^{core} + N_O^{ex} = g_O^{core} N_g + N_O^{ex} \tag{2a}$$

$$N_S^W = N_S^{core} + N_S^{ex} = g_S^{core} N_g + N_S^{ex} \tag{2b}$$

$$N_W^W = N_W^{core} + N_W^{ex} = g_W^{core} N_g + N_W^{ex} \tag{2c}$$

The species balance equations result from the summation of all molecules in the continuous and dispersed phases, and under the maximum term approximation, they can be written as follows:

$$\begin{aligned} N_O &= N_O^O + N_O^I + N_O^W \\ &= N_O^O + g_O^I N_g + g_O^{core} N_g + N_O^{ex} \end{aligned} \tag{3a}$$

$$\begin{aligned} N_S &= N_S^O + N_S^I + N_S^W \\ &= N_S^O + g_S^I N_g + g_S^{core} N_g + N_S^{ex} \end{aligned} \tag{3b}$$

$$N_W = N_W^O + N_W^W = N_W^O + g_W^{core} N_g + N_W^{ex} \tag{3c}$$

The total Gibbs free energy of the solution, G, is the sum of the Gibbs free energy of the continuous phase containing droplets and the excess phase

$$\begin{aligned} G = {} & N_O^O \mu_O^O + N_S^O \mu_S^O + N_W^O \mu_W^O + N_g \mu_g \\ & + N_O^{ex} \mu_O^{ex} + N_S^{ex} \mu_S^{ex} + N_W^{ex} \mu_W^{ex} \end{aligned} \tag{4}$$

dx.doi.org/10.1021/la203909b | Langmuir 2012, 28, 1738−1752

where $\mu_i{}^j$ is the chemical potential of component i in phase j. The expression for the chemical potential of the droplet in the continuous phase containing droplets, μ_g, is given by

$$\mu_g = \mu_g^* + kT[\ln(\gamma_g^* X_g) + U_g^{hs}] \quad (5)$$

where μ_g^* is the standard chemical potential for a droplet that is infinitely dilute in the continuous phase, γ_g^* is the activity coefficient of the droplet in the continuous phase in the infinite dilution reference frame, X_g is the mole fraction of a droplet in the continuous phase, and k is the Boltzmann constant. U_g^{hs} is the nonideality from the hard-sphere droplets.

The standard chemical potential μ_g^* of the aggregate in the continuous phase can be split into a part due to the interfacial layer (denoted by superscript I) and another part due to the disperse water domain of the droplet (denoted by the superscript core) and is given by[3]

$$\mu_g^* = \mu_g^{I*} + g_O^{core}\mu_O^{core} + g_W^{core}\mu_W^{core} + g_S^{core}\mu_S^{core} \quad (6)$$

After substituting eqs 5 and 6 into eq 4, we have

$$\begin{aligned} G = {} & N_O^O\mu_O^O + N_S^O\mu_S^O + N_W^O\mu_W^O \\ & + N_g\{\mu_g^{I*} + g_O^{core}\mu_O^{core} + g_W^{core}\mu_W^{core} \\ & + g_S^{core}\mu_S^{core} + kT[\ln(\gamma_g^* X_g) + U_g^{hs}]\} \\ & + N_O^{ex}\mu_O^{ex} + N_S^{ex}\mu_S^{ex} + N_W^{ex}\mu_W^{ex} \end{aligned} \quad (7)$$

Using $N_O^{core} = N_g g_O^{core}$, $N_W^{core} = N_g g_W^{core}$, and $N_S{}^{core} = N_g g_S^{core}$ and rewriting eq 7, we have

$$\begin{aligned} G = {} & N_O^O\mu_O^O + N_S^O\mu_S^O + N_W^O\mu_W^O + N_g\mu_g^{I*} \\ & + N_g kT[\ln(\gamma_g^* X_g) + U_g^{hs}] + N_O^{core}\mu_O^{core} \\ & + N_S^{core}\mu_S^{core} \\ & + N_W^{core}\mu_W^{core} + N_O^{ex}\mu_O^{ex} + N_S^{ex}\mu_S^{ex} + N_W^{ex}\mu_W^{ex} \end{aligned} \quad (8)$$

Using eq 3b to substitute N_S^{core} into eq 8, we have

$$\begin{aligned} G = {} & N_O^O\mu_O^O + N_S^O\mu_S^O + N_W^O\mu_W^O + N_g\mu_g^{I*} \\ & + N_g kT[\ln(\gamma_g^* X_g) + U_g^{hs}] + N_O^{core}\mu_O^{core} \\ & + (N_S - N_S^O - N_S^{ex} - N_S^I)\mu_S^{core} \\ & + N_W^{core}\mu_W^{core} + N_O^{ex}\mu_O^{ex} + N_S^{ex}\mu_S^{ex} + N_W^{ex}\mu_W^{ex} \end{aligned} \quad (9)$$

For the chemical potentials in the equation above, we use the reference state of the pure species except for the chemical potential of the surfactant in the interfacial layer, which has the reference state in the infinite dilution limit. The expression for the chemical potential with the reference state of the pure species is given by

$$\mu_i^j = \mu_i^o + kT[\ln(\gamma_i^j X_i^j) + U_i^{hs}] \quad (10)$$

where $\mu_i{}^o$ is the standard chemical potential of pure species i, γ_i^j is the activity coefficient of species i in phase j in the pure-state reference frame, and U_i^{hs} is the nonideality from the hard-sphere droplets. U_i^{hs} is different from zero when j represents the dominant component of the continuous phase (i.e., j = O for W/O and j = W for O/W).

The expression for the chemical potential with the infinite dilution reference frame is given by

$$\mu_i^j = \mu_i^{j*} + kT[\ln(\gamma_i^{j*} X_j^i) + U_i^{hs}] \quad (11)$$

where $\mu_i^j{}^*$ is the standard chemical potential for species i that is infinitely dilute in phase j, $\gamma_i^j{}^*$ is the activity coefficient of species i in phase j in the infinite dilution reference frame, and X_i^j is the mole fraction of species i in phase j. Substituting eqs 10 and 11 into eq 9 yields

$$\begin{aligned} G = {} & N_O^O\{\mu_O^o + kT[\ln(\gamma_O^O X_O^O) + U_O^{hs}]\} \\ & + N_S^O\{\mu_S^o + kT[\ln(\gamma_S^O X_S^O) + U_S^{hs}]\} \\ & + N_W^O\{\mu_W^o + kT[\ln(\gamma_W^O X_W^O) + U_W^{hs}]\} \\ & + N_g\{\mu_g^{I*} + kT[\ln(\gamma^*{}_g X_g) + U_g^{hs}]\} \\ & + N_O^{core}[\mu_O^o + kT[\ln(\gamma_O^{core} X_O^{core})] \\ & + (N_S - N_S^O - N_S^{ex})[\mu_S^o + kT\ln(\gamma_S^{core} X_S^{core})] \\ & - N_S^I[\mu_S^{core*} + kT\ln(\gamma_S^{core*} X_S^{core})] \\ & + N_W^{core}[\mu_W^o + kT\ln(\gamma_W^{core} X_W^{core})] \\ & + N_O^{ex}[\mu_O^o + kT\ln(\gamma_O^{ex} X_O^{ex})] \\ & + N_S^{ex}[\mu_S^o + kT\ln(\gamma_S^{ex} X_S^{ex})] \\ & + N_W^{ex}[\mu_W^o + kT\ln(\gamma_W^{ex} X_W^{ex})] \end{aligned} \quad (12)$$

Reorganizing eq 12 using the mass balance equations (eqs 3a−3c) yields

$$\begin{aligned} G = {} & N_O\mu_O^o + N_S\mu_S^o + N_W\mu_W^o - N_O^I\mu_O^o \\ & - N_S^I\mu_S^{core*} + N_g\mu_g^{I*} + N_g kT[\ln(\gamma^*{}_g X_g) \\ & + U_g^{hs}] + N_O^O kT[\ln(\gamma_O^O X_O^O) + U_O^{hs}] \\ & + N_S^O kT[\ln(\gamma_S^O X_S^O) + U_S^{hs}] + N_W^O kT \\ & [\ln(\gamma_W^O X_W^O) + U_W^{hs}] + N_O^{core} kT \\ & \ln(\gamma_O^{core} X_O^{core}) + (N_S^{core} + N_S^I)kT \\ & \ln(\gamma_S^{core} X_S^{core}) - N_S^I kT\ln(\gamma_S^{core*} X_S^{core}) \\ & + N_W^{core} kT\ln(\gamma_W^{core} X_W^{core}) + N_O^{ex} kT \\ & \ln(\gamma_O^{ex} X_O^{ex}) + N_S^{ex} kT\ln(\gamma_S^{ex} X_S^{ex}) + N_W^{ex} kT \\ & \ln(\gamma_W^{ex} X_W^{ex}) \end{aligned} \quad (13)$$

We use the relation provided by Prausnitz et al.[24] for the infinite dilution activity coefficient of a surfactant

$$\gamma_S^{core*} = \frac{\gamma_S^{core}}{\gamma_S^{core*}} \text{ where } \gamma_S^{core\infty} = \lim_{X_S^{core}\to 0} \gamma_S^{core}$$

and then we move to the left side of eq 13 the terms that depend only on fixed variables T, p, N_O, N_S, and N_W. G' is defined as

dx.doi.org/10.1021/la203909b | Langmuir 2012, 28, 1738−1752

$$G' = G - N_O\mu_O^o - N_S\mu_S^o - N_W\mu_W^o$$
$$= -N_O^I\mu_O^o - N_S^I\mu_S^{core*} + N_g\mu_g^{I*} + N_gkT$$
$$[\ln(\gamma_g^*X_g) + U_g^{hs}] + N_O^OkT[\ln(\gamma_O^OX_O^O)$$
$$+ U_O^{hs}] + N_S^OkT[\ln(\gamma_S^OX_S^O) + U_S^{hs}]$$
$$+ N_W^OkT[\ln(\gamma_W^OX_W^O) + U_W^{hs}] + N_O^{core}kT$$
$$\ln(\gamma_O^{core}X_O^{core}) + N_S^{core}kT\ln(\gamma_S^{core}X_S^{core})$$
$$+ N_W^{core}kT\ln(\gamma_W^{core}X_W^{core}) + N_S^IkT$$
$$\ln\gamma_S^{core\infty} + N_O^{ex}kT\ln(\gamma_O^{ex}X_O^{ex}) + N_S^{ex}kT$$
$$\ln(\gamma_S^{ex}X_S^{ex}) + N_W^{ex}kT\ln(\gamma_W^{ex}X_W^{ex}) \quad (14)$$

Reorganizing the total Gibbs free energy equation once more and dividing it by kT, we obtain the working equations for water-in-oil microemulsions

$$\frac{G'}{kT} = N_gg_S^I\frac{\Delta\mu_g^{I*}}{kT} + N_g[\ln(\gamma^*{}_gX_g) + U_g^{hs}]$$
$$+ N_O^O[\ln(\gamma_O^OX_O^O) + U_O^{hs}]$$
$$+ N_S^O[\ln(\gamma_S^OX_S^O) + U_S^{hs}]$$
$$+ N_W^O[\ln(\gamma_W^OX_W^O) + U_W^{hs}] + N_O^{core}$$
$$\ln(\gamma_O^{core}X_O^{core}) + N_S^{core}\ln(\gamma_S^{core}X_S^{core})$$
$$+ N_W^{core}\ln(\gamma_W^{core}X_W^{core}) + N_S^I\ln\gamma_S^{core\infty}$$
$$+ N_O^{ex}\ln(\gamma_O^{ex}X_O^{ex}) + N_S^{ex}\ln(\gamma_S^{ex}X_S^{ex})$$
$$+ N_W^{ex}\ln(\gamma_W^{ex}X_W^{ex}) \quad (15)$$

and

$$\Delta\mu_g^{I*} = \frac{1}{g_S^I}\mu_g^{I*} - \mu_S^{core*} - \frac{g_O^I}{g_S^I}\mu_O^o \quad (16)$$

where $\Delta\mu_g^{I*}$ is the standard free energy due to the transfer of one surfactant molecule at infinite dilution from the aqueous core and g_O^I/g_S^I oil molecules from pure oil to the interfacial layer of the droplet. In eq 6, the droplet is also at infinite dilution.

Oil-in-Water Droplet Microemulsions. Consider the microemulsion system is composed of N_O oil molecules, N_S surfactant molecules, and N_W water molecules at temperature T and pressure p. The oil-in-water microemulsion has a continuous water phase and an upper phase of excess oil. The continuous water phase is composed of N_O^W oil molecules, N_S^W surfactant molecules, N_W^W water molecules, and N_g droplets. The schematic representation of an oil-in-water microemulsions is given in Figure 2.

The interfacial layer is composed of g_O^I oil molecules and g_S^I surfactant molecules, which adds to a total of N_O^I oil molecules and N_S^I surfactant molecules forming the interfacial layer as given in eqs 1a and 1b. We assume that the interfacial layer is free of water molecules ($g_W^I = 0$ and $N_W^I = 0$).

The oil domain within the disperse droplets is composed of g_O^{core} oil molecules, g_S^{core} surfactant molecules, and g_W^{core} water molecules. The excess oil phase is composed of N_O^{ex} oil molecules, N_S^{ex} surfactant molecules, and N_W^{ex} water molecules, summing to a total of N_O^O, N_S^O, and N_W^O oil, surfactant, and water molecules, respectively, in the oil phases.

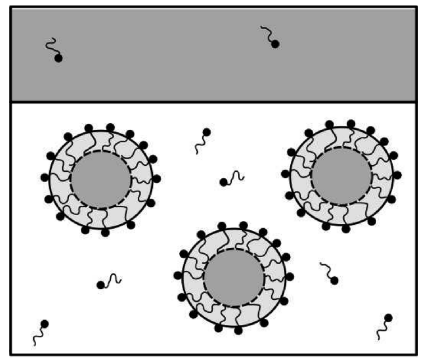

Figure 2. Schematic representation of a two-phase oil-in-water droplet microemulsion.

$$N_O^O = N_O^{core} + N_O^{ex} = g_O^{core}N_g + N_O^{ex} \quad (17a)$$
$$N_S^O = N_S^{core} + N_S^{ex} = g_S^{core}N_g + N_S^{ex} \quad (17b)$$
$$N_W^O = N_W^{core} + N_W^{ex} = g_W^{core}N_g + N_W^{ex} \quad (17c)$$

The species balance equations result from the summation of all molecules in the continuous and dispersed phases, and under the maximum term approximation, they can be written as follows:

$$N_O = N_O^W + N_O^I + N_O^O$$
$$= N_O^W + g_O^IN_g + g_O^{core}N_g + N_O^{ex} \quad (18a)$$

$$N_S = N_S^W + N_S^I + N_S^O$$
$$= N_S^W + g_S^IN_g + g_S^{core}N_g + N_S^{ex} \quad (18b)$$

$$N_W = N_W^W + N_W^O = N_W^W + g_W^{core}N_g + N_W^{ex} \quad (18c)$$

The total Gibbs free energy of the solution, G, is the sum of the Gibbs free energy of the continuous water phase and the excess oil phase:

$$G = N_O^W\mu_O^W + N_S^W\mu_S^W + N_W^W\mu_W^W + N_g\mu_g$$
$$+ N_O^{ex}\mu_O^{ex} + N_S^{ex}\mu_S^{ex} + N_W^{ex}\mu_W^{ex} \quad (19)$$

Substituting the chemical potential of the droplet in the continuous phase in eqs 6 and 11 into eq 19 yields

$$G = N_O^W\mu_O^W + N_S^W\mu_S^W + N_W^W\mu_W^W$$
$$+ N_g\{\mu_g^{I*} + g_O^{core}\mu_O^{core} + g_W^{core}\mu_W^{core}$$
$$+ g_S^{core}\mu_S^{core} + kT[\ln(\gamma_g^*X_g) + U_g^{hs}]\}$$
$$+ N_O^{ex}\mu_O^{ex} + N_S^{ex}\mu_S^{ex} + N_W^{ex}\mu_W^{ex} \quad (20)$$

Using $N_O^{core} = N_gg_O^{core}$, $N_W^{core} = N_gg_W^{core}$, and $N_S^{core} = N_gg_S^{core}$ and rewriting eq 20 yields

$$G = N_O^W\mu_O^W + N_S^W\mu_S^W + N_W^W\mu_W^W + N_g\mu_g^{I*}$$
$$+ N_gkT[\ln(\gamma_g^*X_g) + U_g^{hs}] + N_O^{core}\mu_O^{core}$$
$$+ N_W^{core}\mu_W^{core} + N_S^{core}\mu_S^{core} + N_O^{ex}\mu_O^{ex}$$
$$+ N_S^{ex}\mu_S^{ex} + N_W^{ex}\mu_W^{ex} \quad (21)$$

dx.doi.org/10.1021/la203909b | Langmuir 2012, 28, 1738−1752

Using eq 18b to substitute N_S^W into eq 21, we have

$$\begin{aligned} G = {} & N_O^W\mu_O^W + (N_S - N_S^{core} - N_S^{ex} - N_S^I)\mu_S^W \\ & + N_W^W\mu_W^W + N_g\mu_g^{I*} + N_gkT[\ln(\gamma_g^*X_g) + U_g^{hs}] \\ & + N_O^{core}\mu_O^{core} + N_W^{core}\mu_W^{core} + N_S^{core}\mu_S^{core} \\ & + N_O^{ex}\mu_O^{ex} + N_S^{ex}\mu_S^{ex} + N_W^{ex}\mu_W^{ex} \end{aligned} \quad (22)$$

For the chemical potentials in the equation above, we use the reference state of the pure species (eq 10) except for the chemical potential of the surfactant in the interfacial layer, which has the reference state in the infinite dilution as expressed by eq 11.

$$\begin{aligned} G = {} & N_O^W\{\mu_O^o + kT[\ln(\gamma_O^WX_O^W) + U_O^{hs}]\} \\ & + (N_S - N_S^{core} - N_S^{ex})\{\mu_S^o + kT[\ln(\gamma_S^WX_S^W) \\ & + U_S^{hs}]\} - N_S^I\{\mu_S^{W*} + kT[\ln(\gamma_S^{W*}X_S^W) + U_S^{hs}]\} \\ & + N_W^W\{\mu_W^o + kT[\ln(\gamma_W^WX_W^W) + U_W^{hs}]\} \\ & + N_g\{\mu_g^{I*} + kT[\ln(\gamma^*{}_gX_g) + U_g^{hs}]\} \\ & + N_O^{core}[\mu_O^o + kT\ln(\gamma_O^{core}X_O^{core})] \\ & + N_S^{core}[\mu_S^o + kT\ln(\gamma_S^{core}X_S^{core})] \\ & + N_W^{core}[\mu_W^o + kT\ln(\gamma_W^{core}X_W^{core})] \\ & + N_O^{ex}[\mu_O^o + kT\ln(\gamma_O^{ex}X_O^{ex})] \\ & + N_S^{ex}[\mu_S^o + kT\ln(\gamma_S^{ex}X_S^{ex})] \\ & + N_W^{ex}[\mu_W^o + kT\ln(\gamma_W^{ex}X_W^{ex})] \end{aligned} \quad (23)$$

Reorganizing eq 23 using the mass balance equations (eqs 18a−18c) yields

$$\begin{aligned} G = {} & N_O\mu_O^o + N_S\mu_S^o + N_W\mu_W^o - N_O^I\mu_O^o \\ & - N_S^I\mu_S^{W*} + N_g\mu_g^{I*} + N_gkT[\ln(\gamma^*{}_gX_g) \\ & + U_g^{hs}] + N_O^WkT[\ln(\gamma_O^WX_O^W) + U_O^{hs}] \\ & + (N_S^W + N_S^I)kT[\ln(\gamma_S^WX_S^W) + U_S^{hs}] \\ & - N_S^IkT[\ln(\gamma_S^{W*}X_S^W) + U_S^{hs}] \\ & + N_W^WkT[\ln(\gamma_W^WX_W^W) + U_W^{hs}] \\ & + N_O^{core}kT\ln(\gamma_O^{core}X_O^{core}) \\ & + N_S^{core}kT\ln(\gamma_S^{core}X_S^{core}) \\ & + N_W^{core}kT\ln(\gamma_W^{core}X_W^{core}) \\ & + N_O^{ex}kT\ln(\gamma_O^{ex}X_O^{ex}) + N_S^{ex}kT\ln(\gamma_S^{ex}X_S^{ex}) \\ & + N_W^{ex}kT\ln(\gamma_W^{ex}X_W^{ex}) \end{aligned} \quad (24)$$

We use the relation provided by Prausnitz et al.[24] for the infinite dilution activity coefficient of the surfactant

$$\gamma_S^{W\infty} = \frac{\gamma_S^W}{\gamma_S^{W*}} \text{ where } \gamma_S^{W\infty} = \lim_{X_S^W\to 0}\gamma_S^W$$

and move to the left side of eq 24 the terms that depend only on fixed variables T, p, N_O, N_S, and N_W. G' is defined as follows:

$$\begin{aligned} G' = {} & G - N_O\mu_O^o - N_S\mu_S^o - N_W\mu_W^o \\ = {} & -N_O^I\mu_O^o - N_S^I\mu_S^{W*} + N_g\mu_g^{I*} + N_gkT \\ & [\ln(\gamma_g^*X_g) + U_g^{hs}] + N_O^WkT \\ & [\ln(\gamma_O^WX_O^W) + U_O^{hs}] + N_S^WkT \\ & [\ln(\gamma_S^WX_S^W) + U_S^{hs}] + N_W^WkT \\ & [\ln(\gamma_W^WX_W^W) + U_W^{hs}] + N_S^IkT\ln\gamma_S^{W\infty} \\ & + N_O^{core}kT\ln(\gamma_O^{core}X_O^{core}) + N_S^{core}kT \\ & \ln(\gamma_S^{core}X_S^{core}) + N_W^{core}kT\ln(\gamma_W^{core}X_W^{core}) \\ & + N_O^{ex}kT\ln(\gamma_O^{ex}X_O^{ex}) + N_S^{ex}kT \\ & \ln(\gamma_S^{ex}X_S^{ex}) + N_W^{ex}kT\ln(\gamma_W^{ex}X_W^{ex}) \end{aligned} \quad (25)$$

By reorganizing the total Gibbs free energy equation once more and dividing it by kT, we obtain the working equations for water-in-oil microemulsions:

$$\begin{aligned} \frac{G'}{kT} = {} & N_gg_S^I\frac{\Delta\mu_g^{I*}}{kT} + N_g[\ln(\gamma_g^*X_g) + U_g^{hs}] \\ & + N_O^W[\ln(\gamma_O^WX_O^W) + U_O^{hs}] \\ & + N_S^W[\ln(\gamma_S^WX_S^W) + U_S^{hs}] \\ & + N_W^W[\ln(\gamma_W^WX_W^W) + U_W^{hs}] + N_S^I\ln\gamma_S^{W\infty} \\ & + N_O^{core}\ln(\gamma_O^{core}X_O^{core}) + N_S^{core} \\ & \ln(\gamma_S^{core}X_S^{core}) + N_W^{core}\ln(\gamma_W^{core}X_W^{core}) \\ & + N_O^{ex}kT\ln(\gamma_O^{ex}X_O^{ex}) + N_S^{ex}\ln(\gamma_S^{ex}X_S^{ex}) \\ & + N_W^{ex}\ln(\gamma_W^{ex}X_W^{ex}) \end{aligned} \quad (26)$$

and

$$\Delta\mu_g^{I*} = \frac{1}{g_S^I}\mu_g^{I*} - \mu_S^{W*} - \frac{g_O^I}{g_S^I}\mu_O^o \quad (27)$$

$\Delta\mu_g^{I*}$ represents the standard free energy due to the transfer of one surfactant molecule at infinite dilution from water and g_O^I/g_S^I oil molecules from pure oil to the interfacial layer of the droplet. Equation 27 differs from eq 16 in relation to the phase from which the surfactant molecule is moved to the interfacial layer. For W/O, the surfactant molecule is transferred from the disperse water core, and for O/W, the surfactant molecule is transferred from the continuous water phase. The difference in pressure in the continuous phase and inside the droplets is neglected in this work; we will examine the effect of pressure in future investigations.

To minimize the total Gibbs free energy, we first define the control variables. The independent variables are assigned values in a manner that is controlled by the optimization scheme used and discussed in the Results and Discussion section.

dx.doi.org/10.1021/la203909b | Langmuir 2012, 28, 1738−1752

With specified independent variables, one can readily calculate the geometrical- and compositional-dependent variables. Then, molar fractions, activity coefficients, and free energies of aggregation are computed and used in the working equation to compute the total Gibbs free energy.

Free Energy of Aggregation. In the molecular thermodynamic modeling approach, the free-energy change associated with the formation of the surfactant aggregate at infinite dilution is expressed as the sum of several free-energy contributions, all of which can be computed given the chemical structure of the various components and the solution conditions:[25]

$$\frac{\Delta\mu_g^{I*}}{kT} = \frac{(\Delta\mu_g^{I*})_{trans}}{kT} + \frac{(\Delta\mu_g^{I*})_{def}}{kT} + \frac{(\Delta\mu_g^{I*})_{steric}}{kT} + \frac{(\Delta\mu_g^{I*})_{int}}{kT} + \frac{(\Delta\mu_g^{I*})_{ent}}{kT} + \frac{(\Delta\mu_g^{I*})_{ionic}}{kT} + \frac{(\Delta\mu_g^{I*})_{mix}}{kT} \quad (28)$$

Explicit expressions are presented here for each of the free-energy contributions in terms of the molecular characteristics of the surfactant and the counterion. Detailed discussions of the origin of the following expressions are found in refs 25 and 26.

Transfer of the Surfactant Tail. The transfer free energy relates to the transfer of a surfactant tail in water to the aggregate interfacial layer. The contribution to the free energy of this transfer is estimated by considering the interfacial layer to be like a liquid hydrocarbon. The fact that the interfacial layer differs from a liquid hydrocarbon gives rise to an additional free-energy contribution that is evaluated immediately below.

The transfer free energy of the surfactant tail from water to a liquid hydrocarbon state in the interfacial layer can be estimated from the experimental data of the solubility of hydrocarbons in water. The expressions for the methylene and methyl group contribution to the free energy of transfer of an aliphatic tail from pure water as a function of temperature (in Kelvin) have been estimated by Nagarajan and Ruckenstein:[25]

$$\left(\frac{(\Delta\mu_g^{I*})_{trans}}{kT}\right)_{CH_2} = 5.85 \ln T + \frac{896}{T} - 36.15 - 0.0056T \quad (29)$$

$$\left(\frac{(\Delta\mu_g^{I*})_{trans}}{kT}\right)_{CH_3} = 3.38 \ln T + \frac{4064}{T} - 44.13 - 0.02595T \quad (30)$$

For surfactant tails made up of two hydrocarbon chains, the contribution to the transfer free energy would be smaller than that calculated on the basis of two independent single chains because of intramolecular interactions. Tanford[27] suggested that the second chain of a dialkyl molecule would contribute about 60% of an equivalent single-chain molecule to the transfer free energy.

Packing and Deformation of the Surfactant Tail. The surfactant tails in the aggregate interfacial layer are not in a state identical to that in liquid hydrocarbons. This is because one end of the surfactant tail in the aggregate is constrained to the interface whereas the entire tail has to assume a conformation consistent with the maintenance of a uniform density equal to that of liquid hydrocarbons in the interfacial layer. Consequently, the formation of aggregates is associated with a positive free-energy contribution stemming from the conformational constraints on the surfactant tail.[25] The packing and deformation free-energy expression for spherical aggregates is given by[25]

$$\frac{(\Delta\mu_g^{I*})_{def}}{kT} = \frac{9P\pi^2}{80}\left[\frac{|R_W - R_O|^2}{N_S L^2}\right] \quad (31)$$

where L is the characteristic segment length for the tail (L = 0.46 nm), N_S is the number of segments in the tail of a surfactant ($N_S = l_S/L$, where l_S is the extended length of the tail), and P is the packing factor defined as

$$P = \frac{V_I}{a|R_W - R_O|} \quad (32)$$

where a is the surface area of the droplet in contact with water per surfactant molecule, V_I is the volume of the interfacial layer per surfactant molecule, and R_W and R_O are the radii of water and oil interfaces for the droplet, respectively, as defined in Figure 3.

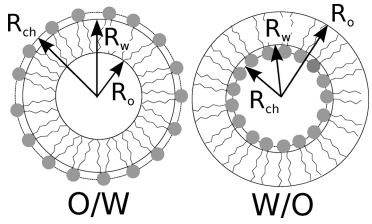

Figure 3. Schematic representation of the radii characterizing the size of W/O and O/W droplets in microemusions.

For surfactant tails with two chains, the tail deformation free energy is the sum of the tail deformation free energy calculated for each chain.

Headgroup Steric Interactions. The steric free-energy contribution accounts for steric interactions between surfactant headgroups and adsorbed counterions at the aggregate interface. The surfactant headgroups and counterions at the interface are treated as components of an ideal localized monolayer[26]

$$\frac{(\Delta\mu_g^{I*})_{steric}}{kT} = -(1 + \sum_j \beta_j)\ln\left(1 - \frac{a_p + \sum_j \beta_j a_{h,j}}{a}\right) \quad (33)$$

where β_j is the degree of binding of counterion j and a_p and $a_{h,j}$ are the effective cross-sectional areas of the hydrated headgroup and hydrated counterion j, respectively. The degree of counterion binding corresponds to the number of counterions of species j adsorbed to the surfactant headgroup per surfactant molecule in the droplet.[26,28]

Besides the well-known dependence of the effective cross-sectional area of the headgroup on the molecular structures of the surfactant headgroup, we account for the effect of the type of counterion on the cross-sectional area of the headgroup at the interfacial layer. The distance between the counterion and the surfactant headgroup depends on the strength of the headgroup−counterion interaction as discussed in our previous work.[28] As an example, the effective cross-sectional area of the hydrated headgroup for surfactant didodecyl dimethylammonium bromide ($(C_{12})_2$DABr) is $a_p = \pi r_p^2$, where r_p = 0.28 nm.

dx.doi.org/10.1021/la203909b | Langmuir 2012, 28, 1738−1752

We use this surfactant later in the article. The cross-sectional area of the counterion is obtained from the hydrated ionic radius and the assumption that it is spherical. The radius of the Br^- counterion is estimated to be 0.118 nm.[29]

Formation of the Aggregate Core–Solvent Interface. The free energy associated with the formation of the interface between the hydrophobic interfacial layer and the aqueous phase is given by[25]

$$\frac{(\Delta\mu_g^{I*})_{int}}{kT} = \frac{\sigma_{agg}}{kT}(a - a_o) \tag{34}$$

where α_{agg} is the macroscopic interfacial tension between the bulk hydrocarbon and the aqueous solution and a_o is the surface area per surfactant molecule shielded from contact with water by the polar headgroup of the surfactant. We assume that the area per surfactant molecule of the core surface shielded from contact with water by the polar headgroup of the surfactant is equal to the effective cross-sectional area of the headgroup ($a_o = a_p$), and a_o can be obtained from the molecular structure of the surfactant headgroup and counterion as discussed above.

The interfacial tension σ_{agg} is calculated in terms of the surface tension σ_S of the aliphatic surfactant tail and the surface tension σ_W of pure water via the relationship interpolated from the experimental data of the water–hydrocarbon interfacial tension:[30,31]

$$\sigma_{agg} = 0.7562(\sigma_S + \sigma_W) - 0.4906(\sigma_S\sigma_W)^{0.5} \tag{35}$$

The surface tension of pure water is given by[32]

$$\sigma_W = 235.8\left(1 - \frac{T}{647.15}\right)^{1.256}\left[1 - 0.625\left(1 - \frac{T}{647.15}\right)\right] \tag{36}$$

where σ_W is expressed in mN/m and the temperature is expressed in Kelvin. The surface tension of normal alkanes is fitted from the experimental data[33]

$$\sigma_S = 29.7003[1 - \exp(-0.1532n_c)] - 0.0896(T - 298.15) \tag{37}$$

where n_c corresponds to the number of carbon atoms in the normal alkane tail.

For double-tailed surfactants, we assume that the surface tension is the average of the surface tension corresponding to each tail ($\sigma_S = (\sigma_{S_nc_1} + \sigma_{S_nc_2})/2$), where $\sigma_{S_nc_1}$ and $\sigma_{S_nc_2}$ are the surface tensions of the normal alkanes corresponding to the two surfactant tails.

Headgroup-Counterion Mixing Entropy. This contribution accounts for the entropic gain associated with mixing of the surfactant heads and the bound counterions at the interface. The surfactant ionic heads and bound counterions are considered to be arranged randomly on the aggregate surface.[26]

$$\frac{(\Delta\mu_g^{I*})_{ent}}{kT} = \ln\left(\frac{1}{1 + \sum_j \beta_j}\right) + \sum_j \beta_j \ln\left(\frac{\beta_j}{1 + \sum_j \beta_j}\right) \tag{38}$$

Headgroup Ionic Interactions. The free energy of the double layer is equal to the amount of work performed in building up the double layer around the colloidal particle by a reversible isothermal process. The ionic free-energy contribution is accounted for by the double-layer free energy of an isolated charged particle[34,35]

$$\frac{(\Delta\mu_g^{I*})_{ionic}}{kT} = \frac{a_{ch}}{kT}\int_o^\sigma \phi_o(\sigma')\, d\sigma' \tag{39}$$

where σ is the surface charge density (charge/area) at the charge surface, ϕ_o is the electrical potential at the aggregate charge surface, and a_{ch} is the surface area per surfactant molecule at the charge surface:

$$a_{ch} = \frac{4\pi R_{ch}^2}{g_S^I} \tag{40}$$

The radius of the charge surface, R_{ch}, is calculated using the radius, R_W, and the distance between the aqueous phase interface and the center of charge of the ionic surfactant head, d_{ch}, as follows (Figure 3):

$$R_{ch} = R_W + d_{ch} \text{ for O/W microemulsions} \tag{41a}$$

$$R_{ch} = R_W - d_{ch} \text{ for W/O microemulsions} \tag{41b}$$

The distance between the aqueous-phase interface and the center of charge of the ionic surfactant head, d_{ch}, is estimated from the molecular structure of the surfactant. For surfactant $(C_{12})_2$DABr, d_{ch} is taken to be 0.1 nm, as for the d_{ch} of alkyl trimethylammoniums.[28]

The integral in eq 39 is the free energy per unit area of the particle surface. The trapezoidal rule may be used for the numerical integration. In this work, we discretize the domain in 20 equally distributed nodes. The charge density is given by

$$\sigma = \frac{e(z_A + \sum_k z_k\beta_k)}{a_{ch}} \tag{42}$$

where e is the elementary charge, z_A is the valence of the surfactant headgroup, and z_k is the valence of counterion k, where k is the number of counterions present in solution. The electrical potential at the surface of charge ϕ_o is determined by solving the Poisson–Boltzmann equation, which in spherical coordinates is given by

$$\frac{d^2\phi}{dx^2} + \frac{2}{x}\frac{d\phi}{dx} = \frac{-e}{\varepsilon_o\varepsilon_{sol}}\sum_j z_j n_j^\infty \exp\left\{-\frac{[z_j e\phi(x) + U_j(x)]}{kT}\right\} \tag{43}$$

In the above equation, ϕ is the self-consistent electrical potential. The electrical potential depends on the spatial distance from the droplet aqueous interface, x. n_j^∞ is the ion concentration infinitely far from the charged interface, and ε_o and ε_{sol} are vacuum permittivity and dielectric constant of the solvent, respectively. The total ionic concentration n_j^∞ is related to the molar concentration c_j^∞ by the relation $n_j^\infty = 10^3 N_{av} c_j^\infty$, where N_{av} is Avogadro's number. U_j is the hard-sphere repulsion that is infinite when the ion is located closer to the surface of charge than the thickness of the Stern layer, $d_{st,j}$

$$U_j(x) = \begin{cases} \infty, & x < R_{ch} + d_{st,j} \\ 0, & x \geq R_{ch} + d_{st,j} \end{cases} \tag{44}$$

dx.doi.org/10.1021/la203909b | *Langmuir* 2012, 28, 1738–1752

We assume that the charged headgroup and the counterions at the Stern layer form solvent-shared ion pairs with different degrees of overlap.[28] The thickness of the Stern layer is estimated from the molecular structure of the hydrated surfactant heads and hydrated counterions and from a knowledge of the qualitative strength of the headgroup−counterion interaction based on the concept of matching water affinities. For headgroup $(C_{12})_2DA^+$ and for counterion Br^- in surfactant $(C_{12})_2DABr$, d_{st} is estimated to be 0.3 nm, as for the d_{st} of alkyl trimethylammonium and bromide.[28]

For pure water at temperatures ranging from 273.15 to 373.15 K,[36]

$$\varepsilon_W = -1.0677 + 306.4670 \exp(-4.52 \times 10^{-3} T) \quad (45)$$

The Poisson−Boltzmann equation is a second-order differential equation with two boundary conditions. One boundary condition is based on the fact that the potential vanishes at infinity (i.e., far away from the charged interface):

$$\lim_{x\to\infty} \phi = 0 \quad (46)$$

At infinity, the derivative of the potential also vanishes:

$$\lim_{x\to\infty} \nabla\phi = 0 \quad (47)$$

The other boundary condition is based on the surface charge. The electrical field or the electrical potential at the charged interface can be fixed. Here, by knowing the surface charge density, we calculate the electrical field at the interface:

$$\nabla\phi|_{x=R_{ch}} = -\frac{\sigma}{\varepsilon_o \varepsilon_W} \quad (48)$$

The Poisson−Boltzmann equation can be solved by finite differences. Spherical discretization is carried out according to Strikwerda.[37] Details of the finite difference method are given in ref 28. The domain is discretized in 100 equally distributed nodes. The domain starts at the distance from the charge surface and increases to up 4 times the Debye length. For an electrolyte solution,

$$\kappa^2 = \frac{\sum_j n_j^\infty (ez_j)^2}{\varepsilon_o \varepsilon_{sol} kT} \quad (49)$$

$1/\kappa$ is the Debye length that is the characteristic length of the electrical double layer. The characteristic length of the solution is about 0.36 nm, which makes the W/O microemulsion droplets with $R_{ch} > 4$ nm large enough for the boundaries described above to be applied.

In previous work,[28] we looked into the counterion effect on the self-assembly of ionic surfactants closely. In that paper, we showed that this description of the ionic electrostatic repulsion properly predicts the critical micelle concentration of both anionic and cationic surfactants of various counterions and the effect of different inorganic salts on the micellization of ionic surfactants.

Mixing Inside the Interfacial Layer. The free-energy contribution of the mixing of surfactant tails and oil molecules in the interfacial layer is estimated using the Flory−Huggins expression, as follows[3]

$$\frac{(\Delta\mu_g^{I*})_{mix}}{kT} = \ln \eta_S + \frac{g_O^I}{g_S^I} \ln \eta_O + \nu_{ST} \frac{(\delta_S^H - \delta_{mix}^H)^2}{kT} + \frac{g_O^I}{g_S^I} \nu_O \frac{(\delta_O^H - \delta_{mix}^H)^2}{kT} \quad (50)$$

where η_S and η_O are the volume fractions of the surfactant tail and oil in the interfacial layer, respectively; ν_{ST} and ν_O are the volumes of the surfactant tail and oil molecule, respectively; δ_S^H and δ_O^H are the Hildebrand solubility parameters of the surfactant tail and the oil, respectively; and δ_{mix}^H is the volume-fraction-averaged solubility parameters of the components in the interfacial layer, $\delta_{mix}^H = \eta_S \delta_S^H + \eta_O \delta_O^H$. The solubility parameters are estimated to be 16.78 $MPa^{1/2}$ for the surfactant tail, 14.93 $MPa^{1/2}$ for *n*-hexane, and 15.34 $MPa^{1/2}$ for *n*-octane.[38,39] The volume fractions of the surfactant tail and oil are readily given by

$$\eta_S = \frac{\nu_{ST}}{\nu_{ST} + (g_O^I/g_S^I)\nu_O} \text{ and } \eta_O = \frac{(g_O^I/g_S^I)\nu_O}{\nu_{ST} + (g_O^I/g_S^I)\nu_O} \quad (51)$$

Geometrical and Compositional Variables. For given control variables N_O, N_S, N_W, T, and p, the global minimum of the total Gibbs free energy, G', defines equilibrium with respect to eight geometrically and compositionally independent variables: g_O^I/g_S^I, a, β, g_O^{core}, g_W^{core}, N_O^O, N_S^O, and N_W^O for water-in-oil microemulsions and g_O^I/g_S^I, a, β, g_O^{core}, g_W^{core}, N_O^W, N_S^W, and N_W^W for oil-in-water microemulsions.

Geometrical Characterization.[3] Both W/O and O/W droplet microemulsions have a core surrounded by an interfacial layer. The interfacial layer excludes the headgroups of the surfactant molecules. Radii R_O and R_W provide the boundaries of the interfacial layer, as represented in Figure 3. The volume of the aggregate can be related to radii R_O and R_W via

$$V_g = \frac{4\pi {R_O}^3}{3} \text{ for W/O droplets} \quad (52)$$

$$V_g = \frac{4\pi {R_W}^3}{3} + g_S^I \nu_{SH} \text{ for O/W droplets} \quad (53)$$

where ν_{SH} is the volume of the polar headgroup of the surfactant.

The volume of the interfacial layer per surfactant molecule V_I is given by

$$V_I = \frac{4\pi}{3g_S^I} |{R_O}^3 - {R_W}^3| = \frac{g_S^I \nu_{ST} + g_O^I \nu_O}{g_S^I} = \nu_{ST} + \frac{g_O^I}{g_S^I} \nu_O \quad (54)$$

The surface area of the droplet in contact with water, per surfactant molecule, is given by

$$a = \frac{4\pi {R_W}^2}{g_S^I} \quad (55)$$

Combining eq 54 and eq 55 yields

$$\frac{R_O}{R_W} = \left(\frac{3V_I}{a|R_O - R_W|} - \frac{3}{4} \right)^{1/2} - \frac{1}{2} \quad (56)$$

dx.doi.org/10.1021/la203909b | *Langmuir* 2012, 28, 1738−1752

The thickness of the interfacial layer is taken to be the surfactant tail length, l_S:

$$|R_O - R_W| = l_S \tag{57}$$

An O/W or a W/O droplet can be characterized by two geometrical variables: (i) the surface area of the droplet in contact with water per surfactant molecule, a, and (ii) the ratio of oil-to-surfactant molecules in the interfacial layer, g_O^I/g_S^I.[3]

Compositional Characterization. In the core, independent variables g_O^{core} and g_W^{core} are used to calculate g_S^{core} using the volume of the core, V_{core}, according to the following relations:

$$V_{core} = \frac{4\pi R_W^3}{3} - g_S^I v_{SH} = g_O^{core} v_O + g_S^{core} v_S + g_W^{core} v_W \text{ for W/O droplets} \tag{58}$$

$$V_{core} = \frac{4\pi R_O^3}{3} = g_O^{core} v_O + g_S^{core} v_S + g_W^{core} v_W \text{ for O/W droplets} \tag{59}$$

In the continuous phase, independent variables N_O^O, N_S^O, and N_W^O or N_O^W, N_S^W, and N_W^W are used to calculate N_g and the composition of the excess phase, N_O^{ex}, N_S^{ex}, and N_W^{ex}, by solving a linear system of equations consisting of the mass balance equations and the total volume, V_{total}:

$$V_{total} = N_O v_O + N_S v_S + N_W v_W = (N_O^O + N_O^{ex}) v_O + (N_S^O + N_S^{ex}) v_S + (N_W^O + N_W^{ex}) v_W + N_g V_g \text{ for W/O droplets} \tag{60}$$

$$V_{total} = N_O v_O + N_S v_S + N_W v_W = (N_O^W + N_O^{ex}) v_O + (N_S^W + N_S^{ex}) v_S + (N_W^W + N_W^{ex}) v_W + N_g V_g \text{ for O/W droplets} \tag{61}$$

The volumes of water and normal alkanes are computed from their liquid densities.[40] The volume of the components at 25 °C are given in Table 1.

Table 1. Volume of the Components at 25 °C

component	v (nm^3)
n-hexane	$v_O = 0.2181$
n-octane	$v_O = 0.2713$
water	$v_W = 0.0301$
surfactant	$v_S = 0.7126$

Constraints. From eq 56 we have the geometrical constraint

$$\left(\frac{3V_I}{a|R_O - R_W|} - \frac{3}{4}\right)^{1/2} > \frac{1}{2} \tag{62}$$

that gives the first geometrical constraint

$$\frac{|R_O - R_W|}{3} - \frac{v_{ST} + (g_O^I/g_S^I) v_O}{a} < 0 \tag{63}$$

There is also a geometrical constraint on the maximum packing density of the droplets. Computer simulations by Finney[41] have confirmed that the maximum packing density (volume fraction of spheres) is approximately 0.64 in the random close-packed limit. Therefore, we assume that

$$\frac{N_g V_g}{N_g V_g + N_O^O v_O + N_S^O v_S + N_W^O v_W} \le 0.64 \text{ for W/O droplets} \tag{64}$$

$$\frac{N_g V_g}{N_g V_g + N_O^W v_O + N_S^W v_S + N_W^W v_W} \le 0.64 \text{ for O/W droplets} \tag{65}$$

We also have the compositional constraints on N_g, N_W^{ex}, N_S^{ex}, N_O^{ex}, and g_S^{core} that they cannot be negative:

$$N_g \ge 0 \tag{66}$$

$$N_W^{ex} \ge 0 \tag{67}$$

$$N_S^{ex} \ge 0 \tag{68}$$

$$N_O^{ex} \ge 0 \tag{69}$$

$$g_S^{core} \ge 0 \tag{70}$$

Hard-Sphere Droplet Interactions. The droplets in the continuous phase give rise to osmotic pressure in the microemulsion. The chemical potential of the species in the continuous phase, other than the droplets, can be calculated in terms of the osmotic pressure Π of a hard-sphere suspension[3]

$$\mu_i(\phi_g) = \mu_i(\phi_g = 0) - \Pi v_i \tag{71}$$

where ϕ_g is the volume fraction of droplets in solution and v_i is the volume of component i.

Carnahan and Starling[42] proposed a semiempirical expression for hard-sphere solutions. The Carnahan–Starling approximation for hard spheres has been used with success in the light-scattering experiments of oil-in-water microemulsions.[43] The Carnahan–Starling equation of state provides the osmotic pressure expression:

$$\Pi = kT\frac{\phi_g}{V_g}\frac{1 + \phi_g + \phi_g^2 - \phi_g^3}{(1 - \phi_g)^3} \tag{72}$$

Using the Carnahan–Starling approximation for osmotic pressure in eq 71, one can write the expression for nonideality from the hard-sphere droplets, U_i^{hs}:[3]

$$U_i^{hs} = v_i\frac{\phi_g}{V_g}\frac{(1 + \phi_g + \phi_g^2 - \phi_g^3)}{(1 - \phi_g)^3} \text{ for } i = \text{O, W, S} \tag{73}$$

The nonideality from the hard-sphere droplets for the droplet, U_g^{hs}, can be derived by using the Gibbs–Duhem relation:[3,44]

$$U_g^{hs} = \ln\left(\frac{\phi_g/V_g}{X_g \sum_{i \ne g} \phi_i/v_i}\right) + \frac{\phi_g(7 - 3\phi_g - \phi_g^2)}{(1 - \phi_g)^2} \tag{74}$$

dx.doi.org/10.1021/la203909b | *Langmuir* 2012, 28, 1738–1752

The mole fraction and volume fraction of species i are related via the expressions

$$X_i = \frac{\phi_i/\nu_i}{\sum \phi_j/\nu_j} \text{ and } \phi_i = \frac{X_i\nu_i}{\sum X_j\nu_j} \quad (75)$$

Activity Coefficient Model. The activity coefficients in our model describe the water and surfactant solubility in oil and the oil and surfactant solubility in water. The mutual solubility of a ternary system is not readily available for most of the systems in which we are interested. Because of the lack of data, we use the binary mutual solubility in our calculations. We assume that the third-component effect on the mutual binary solubility can be neglected. For water and oil mutual solubility, we use the UNIQUAC model, and for surfactants in oil and in water, we use the two-suffix Margules model. For the droplets in the continuous phase, we assume that γ_g^* is equal to 1. In this work, the prediction from our model centers on the ternary system of water, a normal alkane, and a surfactant. The activity coefficients for these systems are given next.

Water and Normal Alkane. For water and normal alkane mutual solubility, we use the UNIQUAC model for the activity coefficient. The expressions can be found in ref 45. The UNIQUAC parameters for (1) water and (2) two normal alkanes are given in Table 2.[46]

Table 2. UNIQUAC Parameters for (1) Water and (2) *n*-Hexane and *n*-Octane[46,a]

n-alkane	r_2	q_2	a_{12}	a_{21}
n-hexane	4.4998	3.856	572.51	1297.1
n-octane	5.8486	4.936	567.29	1271.4

[a]For water, r_1 = 0.92 and q_1 = 1.4.

Surfactant. For the activity coefficient of surfactant in oil and surfactant in water, we use the two-suffix Margules model, assuming a pseudobinary system of water and surfactant for the aqueous phase and oil and surfactant for the oil phase. For a binary system, we can write

$$\ln \gamma_1 = \frac{A}{RT}x_2^2 \quad (76)$$

$$\ln \gamma_2 = \frac{A}{RT}x_1^2 \quad (77)$$

At infinite dilution,

$$\gamma_1^\infty \equiv \lim_{x_1\to 0} \gamma_1 = \exp\left(\frac{A}{RT}\right) \quad (78)$$

$$\gamma_2^\infty \equiv \lim_{x_2\to 0} \gamma_2 = \exp\left(\frac{A}{RT}\right) \quad (79)$$

In the above expressions, A is the parameter of the activity coefficient model and R is the gas constant. For the surfactant infinitely diluted in water and in oil, we estimate the infinite dilution activity coefficient via the relation[47]

$$\gamma_S^{W\infty} = \mathrm{cmc}_W^{-1} \quad (80)$$

$$\gamma_S^{O\infty} = \mathrm{cmc}_O^{-1} \quad (81)$$

where cmc_W and cmc_O are the critical micelle concentrations (cmc's) of the surfactant in water and in oil, respectively. The cmc of DDABr in water is cmc_W = 0.37 mM, and that for DDABr in *n*-heptane is cmc_O = 0.28 mM.[48]

The activity coefficient expressions used for surfactant, oil, water, and droplets satisfy the Gibbs–Duhem equation. The nonideality term from the hard-sphere droplets is based on the Gibbs–Duhem equation. For water and oil mutual solubility, we assume that the surfactant concentration in water and oil phases is negligible, and we use the UNIQUAC model for the activity coefficient. The UNIQUAC parameters for water and normal alkanes used satisfy the Gibbs–Duhem relation. The only terms left are the ones for the surfactant in oil and surfactant in water. Because of a small amount of surfactant in water and in oil, these terms are numerically zero.

RESULTS AND DISCUSSIONS

In this section, we will first present the results of our micellization model described in ref 28 for an ionic double-tailed surfactant in water. In ref 28, we considered only single-tailed surfactants. Complexities in minimizations of the Gibbs free energy of microemulsion systems are addressed next. The successful use of the particle swarm optimization in the minimization of the Gibbs free energy function that has an unusual number of minima is then presented for the ternary mixture of surfactant, water, and normal alkanes. The composition of the phases and the number of droplets in the water-in-oil microemulsion from the global minimum of the Gibbs free energy are discussed. We also present the polydispersity of microemulsions and explain how to assess the polydispersity by taking advantage of the stochasticity of the optimization method. The computed droplet size of two different normal alkanes is compared with the measured data. All of the computations are made at 25 °C.

cmc for DDABr in Water. In this work, we investigate the droplet-type microemulsion formed by the DDABr surfactant. As a first step, we verify the aggregation of DDABr molecules in water and the cmc on the basis of the headgroup molecular parameters presented for this double-tailed surfactant. We use the micellization model discussed in ref 28.

In Figures 4 and 5, we compare the calculated $C_{12}C_N$DABr and $C_{14}C_N$DABr cmc values in water with the experimental

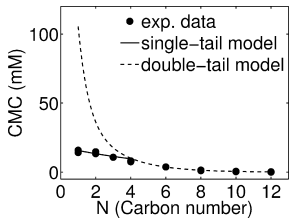

Figure 4. cmc of $C_{12}C_N$DABr in water at 25 °C.

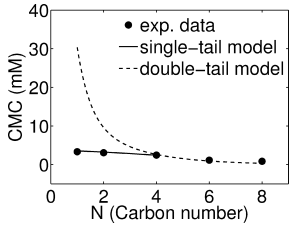

Figure 5. cmc of $C_{14}C_N$DABr in water at 25 °C.

data[49−53] at 25 °C. We use the free energy of the micellization model and molecular parameters provided in the Free Energy

dx.doi.org/10.1021/la203909b | Langmuir 2012, 28, 1738−1752

of Aggregation section. The results in Figures 4 and 5 show that for carbon tails with less than four carbons the single-tailed model works well. When the carbon tail number exceeds four, the single-tailed model becomes inaccurate and the algorithm runs into convergence problems. In these plots, we find that the double-tailed model is a powerful algorithm when the second tail has at least four carbons.

The surfactant we use in the following subsections has two tails with 12 carbons each. Therefore, the double-tailed model adequately describes the aggregation of this surfactant.

Energy-Minimization Strategy. Now that we have examined the free energy of aggregation to the surfactant of interest and confirmed that the double-tailed model adequately describes the aggregation of DDABr, we perform the total Gibbs free energy minimization for the microemulsion expression derived in this work.

To minimize the total Gibbs free energy, we use the particle swarm optimization (PSO) method. The PSO is a heuristic optimization method proposed by Kennedy and Eberhart.[54] Random values are used as initial estimates for each of the independent variables, satisfying the restrictions described above. We have implemented the PSO algorithm as proposed by Schwaab et al.[55] One of the main advantages of using the PSO method is the large phase space of the independent variables searched without encountering numerical difficulties. One of the main disadvantages of the heuristic optimization methods is that, in general, they are slower than the deterministic ones.

Initially, we used the direct optimization FFSQP method[56] to minimize the total Gibbs free energy; the FFSQP method failed with prohibitive numerical problems. We have found that the objective function is not a smooth function of the independent variables; therefore, the FFSQP cannot find the direction of search via its derivative methods. We also used the FFSQP at the end of the PSO optimization, and the FFSQP failed to improve the minimum found by the PSO.

For completeness, we used the stochastic PSO and deterministic FFSQP methods to minimize the Gibbs free energy for the micelle model. And for this simpler system, both stochastic and deterministic approaches converge to the same result.

In Figure 6, we present the Gibbs free energy function from eq 15 versus two independent variables (a and g_O^I/g_S^I) while holding the other independent variables constant. The values of independent variables β, g_O^{core}, g_W^{core}, N_O^O, N_S^O, and N_W^O are given. The areas in white in Tables 3 and 4 correspond to the region for which the Gibbs free energy is not defined for the independent variables because of the constrains. Figure 6a clearly reveals that the direct methods that require smooth functions cannot be used to minimize this objective function. Figure 6b shows an unusual number of local minima and high ruggedness in the Gibbs free energy function.

Because of the fact that the optimization method used is heuristic, for each composition we repeat the Gibbs free energy minimization a large number of times. For this work, we set the number of searching points to 20. For each given overall composition, we perform at least 1000 runs. As an example, in Figure 7 we provide the results for 100 runs for the overall composition of a 66/20/14 weight ratio of *n*-hexane/water/DDABr. The run that corresponds to the global minimum of the Gibbs free energy is marked in the plots as open squares.

For each PSO run, we generate new initial estimates for the independent variables using a random number generator. In Figure 7, we observe that the PSO runs do not depend on the result of the previous run. The plots of the independent

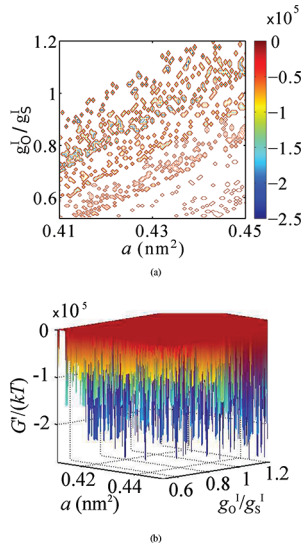

Figure 6. (a) Contour and (b) surface plots showing the roughness of the Gibbs free energy surface. The color map represents $G'/(kT)$. The overall composition and the fixed independent variables are given in Tables 3 and 4.

Table 3. Compositional Features at the Global Minimum of the Gibbs Free Energy for the Overall Composition of the 66/20/14 Weight Ratio of *n*-Hexane/Water/DDABr

overall composition
N_O = 612 704
N_W = 29 263
N_S = 888 134
composition of the continuous oil phase
N_g = 32
N_O^O = 572 872.1
N_W^O = 11 408.7
N_S^O = 83.3
composition of the interfacial layer
g_S^I = 910.3
g_O^I = 1243.3
composition of the aqueous core
g_O^{core} = 1.37
g_W^{core} = 25 888.4
g_S^{core} = 1.54
composition of the excess phase
N_O^{ex} = 1.93
N_W^{ex} = 48 296.2
N_S^{ex} = 0.984

variables versus the PSO run number give results similar to those in Figure 7.

To investigate the dependence on the total number of molecules, we increase the total number of molecules and perform 1000 PSO runs for each composition. The results show that the search for the total Gibbs free energy minimum for a larger total number molecules takes longer, but the global minima of the Gibbs free energy for both set of runs are comparable and the geometrical and compositional features remain the same.

Global Minima of the Gibbs Free Energy. When we plot the minima of Gibbs free energy versus the independent variables for a large number of PSO runs, we observe the global minimum in the Gibbs free energy for each independent

dx.doi.org/10.1021/la203909b | *Langmuir* 2012, 28, 1738−1752

Table 4. Geometrical Features at the Global Minimum of the Gibbs Free Energy for the Overall Composition of the 66/20/14 Weight Ratio of *n*-Hexane/Water/DDABr

droplet radii
R_O = 7.403 nm
R_W = 5.735 nm
interfacial layer
a = 0.4541 nm^2
g^I_O/g^I_S = 1.3658
degree of ion adsorption
β = 0.736
volumes
V_g = 1 699.6 nm^3
V_{core} = 779.7 nm^3
V_{total} = 181 205 nm^3

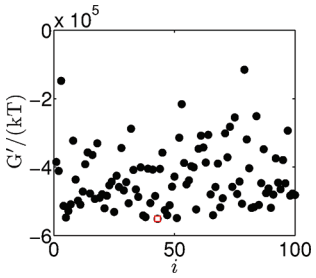

Figure 7. Minima in the total Gibbs free energy vs the PSO run number. The open square corresponds to the global minimum in the Gibbs free energy among 100 PSO runs for the overall composition of the 66/20/14 weight ratio of *n*-hexane/water/DDABr.

variable as expected. Figure 8 depicts the result for 100 PSO runs for the surface area of the droplet in contact with water per

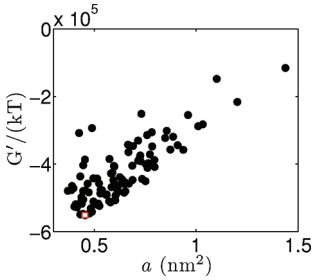

Figure 8. Minima in the total Gibbs free energy vs a. The open square corresponds to the global minimum in the Gibbs free energy among 100 PSO runs for the overall composition of the 66/20/14 weight ratio of *n*-hexane/water/DDABr.

surfactant molecule, a. For the given overall composition, the global minimum in the total Gibbs free energy corresponds to a = 0.454 nm^2, and in Figure 9, we have the result for 100 PSO runs for the ratio g^I_O/g^I_S when the global minimum corresponds to g^I_O/g^I_S = 1.366.

In Figure 10, we observe that the global minimum in the Gibbs free energy with respect to β is not well defined, as it is for a and g^I_O/g^I_S. However, as the number of PSO runs increases, the global minimum becomes well defined for all independent variables.

Microstructure and Composition. In Figure 11, we plot the minimum in the total Gibbs free energy versus the radius of

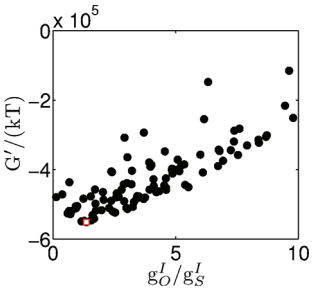

Figure 9. Minima in the total Gibbs free energy versus g^I_O/g^I_S. The open square corresponds to the global minimum in the Gibbs free energy among 100 PSO runs for the overall composition of the 66/20/14 weight ratio of *n*-hexane/water/DDABr.

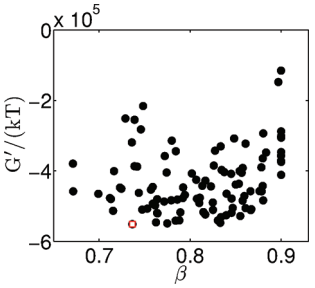

Figure 10. Minima in the total Gibbs free energy vs β. The open square corresponds to the global minimum in the Gibbs free energy among 100 PSO runs for the overall composition of the 66/20/14 weight ratio of *n*-hexane/water/DDABr.

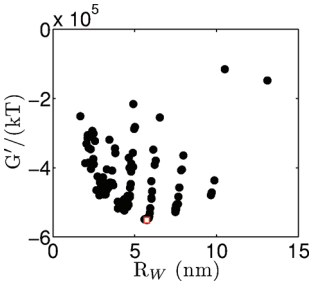

Figure 11. Minima in the total Gibbs free energy vs R_W. The open square corresponds to the global minimum in the Gibbs free energy among 100 PSO runs for the overall composition of the 66/20/14 weight ratio of *n*-hexane/water/DDABr.

the aqueous core for 100 PSO runs. The global minimum of the total Gibbs free energy corresponds to the radius of the aqueous core, which is equal to 5.73 nm. Droplets that are smaller or larger than 5.73 nm have a higher Gibbs free energy.

Figure 12 shows the minimum in the total Gibbs free energy versus the number of droplets for 100 PSO runs. There are around 32 droplets at the global minimum, which gives a volume fraction of droplets in the continuous oil phase of 30%.

The total number of molecules for each component defined for each overall composition is large enough that the system can arrange to form a significant number of aggregates. By using our minimization strategy, in Figure 12 we see that a configuration with as many as 500 droplets has been evaluated.

Tables 3 and 4 present compositional and geometrical results corresponding to the global minimum marked in Figures 7−12 for the overall composition of the 66/20/14 weight ratio of *n*-hexane/water/DDABr. Table 3 provides the compositional outcomes of the global minimization. The results show that the

dx.doi.org/10.1021/la203909b | *Langmuir* 2012, 28, 1738−1752

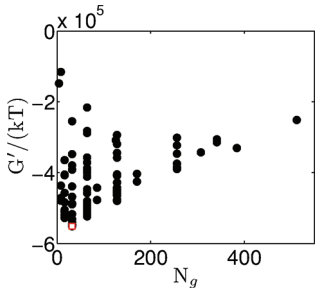

Figure 12. Minima in the total Gibbs free energy vs the number of droplets. The open square corresponds to the global minimum in the Gibbs free energy among 100 PSO runs for the overall composition of the 66/20/14 weight ratio of *n*-hexane/water/DDABr.

continuous oil phase is composed mostly of oil, with a small mole fraction of droplets, water, and surfactant. The aqueous core and the excess phase are composed mostly of water and trace amounts of surfactant and oil. Although g_O^{core} is very small for W/O microemulsions, it is different from zero. This low solubility of oil in water is an important aspect of the phase-equilibrium calculation. If water and oil would be completely insoluble, some of the interesting features of microemulsions may not be observed. The geometrical outcomes of the minimization are given in Table 4. The results provide the size of the droplets and the composition of the interfacial layer.

The results in Tables 3 and 4 correspond to the global minimum in the total Gibbs free energy, but as we will discuss in the next section, microemulsion systems are polydisperse. As a result of the polydispersity, it is expected that the specific values of the number of molecules in each phase given in the tables above undergo variation; however, the general behavior of the predominance of oil molecules in the oil phase and the predominance of water molecules in the water phase should remain unchanged.

Droplet Size Distribution. It has been experimentally verified by different analytical techniques that microemulsions are, in fact, polydisperse.[57] Moreover, it has been observed that the reported polydispersity of microemulsion droplets depends on the experimental technique. For example, the polydispersity measured by dynamic light scattering is much less than that measured by elastic light scattering or neutron scattering.[58]

Our results support the evidence that microemulasions are polydisperse systems. In Figure 11, we observe that for very similar Gibbs free energies the droplets may have different radii. The polydispersity of the microemulsions can be obtained by traditional methods such as the one proposed by Nagarajan and Ruckenstein.[3] For the calculation of the size distribution of the microemulsion droplets, one can take advantage of the stochasticity of the PSO optimization method and use the Monte Carlo approach to calculate the size distribution of the droplets. The central idea of the Monte Carlo methods is to use random samples of inputs to explore the behavior of a complex system or process by scanning a phase space with multiple dimensions. In our methodology, the algorithm may sample anywhere within set limits, but the result is statistically directed toward the minimum by the PSO.

After performing the PSO minimization for a given overall composition a large number of times, we use the Gibbs measure to calculate the average of the aqueous core radius of the droplets. The Gibbs measure is a probability measure associated with the Boltzmann distribution that generalizes the notion of the canonical ensemble. The Gibbs measure is a natural mathematical description of an equilibrium state of a physical system that consists of a very large number of interacting components, or in probabilistic terms, a Gibbs measure is the distribution of a countably infinite family of random variables that admit some prescribed conditional probabilities.[59]

Using the Gibbs measure, we can calculate the average of the aqueous core radius of the droplets from

$$\bar{R}_W = \frac{\sum R_W e^{-G'/(kT)}}{\sum e^{-G'/(kT)}} \tag{82}$$

For example, for the overall composition of the 66/20/14 weight ratio of *n*-hexane/water/DDABr the average of the aqueous core radius of the droplets is found to be 5.35 nm whereas the global minimum in the total Gibbs free energy gives a radius of 5.73 nm.

Comparison with Experimental Data. In a series of papers, Ninham et al. have investigated the three-component microemulsions of surfactant DDABr.[14−20] In an investigation on the structure and dynamics of DDABr/water/alkanes, Blum et al.[18] provide phase diagrams for DDABr, water, and alkanes showing the region of bicontinuous and water-in-oil droplet microemulsions. Using X-ray techniques, they also have estimated the size of the microemulsion droplets, given in Table 5.[14] Because basic data of the phase diagram are not provided, we compare the results from our model for size of the droplets with experimental data in terms of the trend and the order of magnitude.

Table 5. Experimental Radius of the Aqueous Core of the W/O Microemulsion Droplet, R_W[14]

n-alkane	R_W (nm)
n-hexane	4.1
n-octane	5.7

In this work, we focus on the water-in-oil droplet microemulsions formed in the ternary systems according to the experimental data by Chen et al.[14] From the phase diagrams for DDABr/water/*n*-hexane provided by these authors,[14] we extract the overall compositions for the water-in-oil droplet microemulsion. We perform Gibbs free energy minimizations for each of these selected overall compositions given in Table 6.

Table 6. Overall Composition in Weight Percent for Water/*n*-Hexane/DDABr

n-hexane	water	DDABr
30	42	28
33	40	27
42	35	23
50	30	20
59	25	16
66	20	14
73	15	12
78	13	9
82	10	8
90	5	5
95	2	3

For each overall composition, we perform a minimum of 1000 PSO runs. In Figure 13, we plot the radius corresponding to the global minimum of the total Gibbs free energy for each

dx.doi.org/10.1021/la203909b | *Langmuir* 2012, 28, 1738−1752

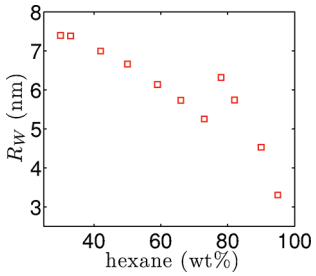

Figure 13. Red squares correspond to the radii of the aqueous droplet core at the global minimum in the Gibbs free energy among 1000 PSO runs.

overall composition. The general trend points to the fact that the aqueous core radius increases as the fraction of water in the system increases. We also observe a discontinuity that we investigate further. The computed radius of the aqueous droplet core falls in the range of the experimentally estimated radius (~4 nm) for the *n*-hexane-rich overall compositions.[14]

To investigate the discontinuity further, we plot in Figure 14 the 10 minima of the 1000 PSO repetitions for each overall composition. In this figure, we observe that the radii lie on two different slopes. We mark the radius corresponding to the global minimum in red squares and apply a color scheme of a different marker for each slope in order to facilitate the analysis.

At higher oil fractions, the slope is steeper (blue upward-pointing triangles), and as the water and surfactant fractions increase, the minimum moves to a less-steep slope (green circles). In the region around the discontinuity, some minima lie on one slope and other minima lie on the other slope for the same composition. Despite noticeable differences in size, these systems have a very small difference in the total Gibbs free energy. We plot the total Gibbs free energy for these systems from Figure 14, and we see that for each composition there is

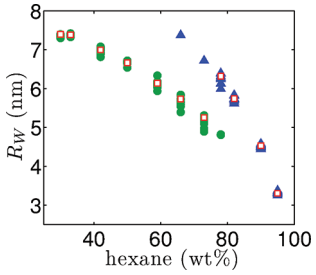

Figure 14. Radii of the aqueous droplet core for the 10 minima in the Gibbs free energy among 1000 PSO runs for each overall composition. The red squares correspond to the radius of the aqueous droplet core at the global minimum in the Gibbs free energy among 1000 PSO runs.

only a small difference in the total Gibbs free energy (plot omitted for the sake of brevity). In line with experimental data, our calculations may indicate that the microemulsion systems are polydisperse for very similar total Gibbs free energy results in droplets of different sizes.

In this work, we have focused on water-in-oil droplet microemulsion for the ternary system. However, this system may need to be revisited once the model for bicontinuous microemulsions is developed. Some of the discontinuities that we calculate using the droplet-type microemulsion model may become smooth with the complete model.

Table 7. Overall Compositions in Weight Percent for Water/*n*-Octane/DDABr

n-octane	water	DDABr
27	50	23
32	47	21
40	41	19

We also select three overall compositions (Table 7) from the phase diagrams for DDABr/water/*n*-octane provided by Chen et al.[14] and perform Gibbs free energy minimizations. The minimization shows that the radius of the aqueous droplet core for the selected overall compositions ranges between 8.2 and 8.5 nm.

Let us compare the droplet size of mixtures containing between 27 and 40 wt % *n*-hexane and *n*-octane. In *n*-octane-containing systems, the radius of the aqueous droplet core is between 8.2 and 8.5 nm; *n*-hexane-containing systems have a radius of the aqueous droplet core that is between 7 and 7.4 nm (Figure 13). Consistent with experimental data (Table 5), the results indicate that the system containing *n*-octane promotes larger droplets than the system containing *n*-hexane.

CONCLUDING REMARKS

In this article, we have developed a molecular thermodynamic theory for droplet-type microemulsions. We derive a theoretical formulation for three-component microemulsions that predicts the structural and compositional features of microemulsions. In the future, we intend to develop a unified thermodynamic model for four- and five-component and bicontinuous microemulsions.

For the minimization scheme, we use the particle swarm optimization method to minimize the total Gibbs free energy. We chose this heuristic optimization method over the direct optimization method because of the unusual number of local minima and the ruggedness of the Gibbs free energy function. One may interpret the extreme ruggedness of the Gibbs free energy function with respect to the polydispersity of the microemulsions.

For a demonstration of predictions from our proposed model, we have selected double-tailed surfactant DDABr that forms water-in-oil droplet microemulsions. The ternary system consists of water, alkane, and DDABr. Computations are performed for two different alkanes: *n*-hexane and *n*-octane. For these systems, there is experimental data available to which we compare the computed results.

The results indicate that the system containing *n*-octane promotes larger droplets than the system containing *n*-hexane, in agreement with experimental data. The computed radius of the aqueous droplet core falls in the range of the measured radius.

AUTHOR INFORMATION

Corresponding Author

*E-mail: abbas.firoozabadi@yale.edu.

ACKNOWLEDGMENTS

We thank the member companies of the Reservoir Engineering Research Institute (RERI) in Palo Alto, CA for financial support.

REFERENCES

(1) Paul, B. K.; Moulik, S. P. *Curr. Sci.* **2001**, *80*, 990−1001.

(2) Fanun, M. *Microemulsions: Properties and Applications*; Surfactant Science Series; CRC Press: Boca Raton, FL, 2009; Vol. *144*.
(3) Nagarajan, R.; Ruckenstein, E. *Langmuir* **2000**, *16*, 6400−6415.
(4) Rossen, W. R.; Brown, R. G.; Davis, H. T.; Prager, S.; Scriven, L. E. *Soc. Pet. Eng. J.* **1982**, *22*, 945−961.
(5) Kilpatrick, P. K.; Scriven, L. E.; Davis, H. T. *Soc. Pet. Eng. J.* **1985**, *25*, 330−342.
(6) García-Sánchez, F.; Eliosa-Jiménez, G.; Salas-Padrón, A.; Hernández-Garduza, O.; Ápam-Martínez, D. *Chem. Eng. J.* **2001**, *84*, 257−274.
(7) Ruckenstein, E. *Fluid Phase Equilib.* **1985**, *20*, 189−206.
(8) Verhoeckx, G. J.; de Bruyn, P. L.; Overbeek, J. T. G. *J. Colloid Interface Sci.* **1987**, *119*, 409−421.
(9) Overbeek, J. T. G.; Verhoeckx, G. J.; de Bruyn, P. L.; Lekkerkerker, H. N. W. *J. Colloid Interface Sci.* **1987**, *119*, 422−441.
(10) Lam, A. C.; Falk, N. A.; Schechter, R. S. *J. Colloid Interface Sci.* **1987**, *120*, 30−41.
(11) Peck, D. G.; Schechter, R. S.; Johnston, K. P. *J. Phys. Chem.* **1991**, *95*, 9541−9549.
(12) Borkovec, M. *Adv. Colloid Interface Sci.* **1992**, *37*, 195−217.
(13) Kumar, P., Mittal, K. L., Eds.; *Handbook of Microemulsion Science and Technology*; Marcel Dekker: New York, 1999.
(14) Chen, S. J.; Evans, D. F.; Ninham, B. W.; Mitchell, D. J.; Blum, F. D.; Pickup, S. *J. Phys. Chem.* **1986**, *90*, 842−847.
(15) Angel, L. R.; Evans, D. F.; Ninham, B. W. *J. Phys. Chem.* **1983**, *87*, 538−540.
(16) Chen, S. J.; Evans, D. F.; Ninham, B. W. *J. Phys. Chem.* **1984**, *88*, 1631−1634.
(17) Ninham, B. W.; Chen, S. J.; Evans, D. F. *J. Phys. Chem.* **1984**, *88*, 5855−5857.
(18) Blum, F. D.; S. Pickup, B. N.; Chen, S. J.; Evans, D. F. *J. Phys. Chem.* **1985**, *89*, 711−713.
(19) Fontell, K.; Ceglie, A.; Lindman, B.; Ninham, B. W. *Acta Chem. Scand. A* **1986**, *40*, 247−256.
(20) Evans, D. F.; Mitchell, D. J.; Ninham, B. W. *J. Phys. Chem.* **1986**, *90*, 2817−2825.
(21) Olla, M.; Monduzzi, M.; Ambrosone, L. *Colloids Surf., A***1999**, *160*, 23−36.
(22) Eicke, H.-F.; Markovic, Z. *J. Colloid Interface Sci.* **1981**, *79*, 151−158.
(23) Zulauf, M.; Eicke, H.-F. *J. Phys. Chem.* **1979**, *83*, 480−486.
(24) Prausnitz, J. M.; Lichtenthaler, R. N.; de Azevedo, E. G. *Molecular Thermodynamics of Fluid-Phase Equilibria*, 2nd ed.; Prentice-Hall: Englewood Cliffs, NJ, 1986.
(25) Nagarajan, R.; Ruckenstein, E. *Langmuir* **1991**, *7*, 2934−2969.
(26) Srinivasan, V.; Blankschtein, D. *Langmuir* **2003**, *19*, 9932−9945.
(27) Tanford, C. *The Hydrophobic Effect: Formation of Micelles and Biological Membranes*, 2nd ed.; Wiley: New York, 1980; Vol. *1*.
(28) Moreira, L.; Firoozabadi, A. *Langmuir* **2010**, *26*, 15177−15191.
(29) Nightingale, E. R. Jr. *J. Phys. Chem.* **1959**, *63*, 1381−1387.
(30) Aveyard, R.; Haydon, D. A. *Trans. Faraday Soc.* **1965**, *61*, 2255−2261.
(31) Zeppieri, S.; Rodríguez, J.; de Ramos, A. L. L. *J. Chem. Eng. Data* **2001**, *46*, 1086−1088.
(32) Vargaftik, N. B.; Volkov, B. N.; Voljak, L. D. *J. Phys. Chem. Ref. Data* **1983**, *12*, 817−820.
(33) Janczuk, B.; Bialopiotrowicz, T.; Wojcik, W. *Colloids Surf.* **1989**, *36*, 391−403.
(34) Derjaguin, B. V. *Trans. Faraday Soc.* **1940**, *36*, 203−215.
(35) Verwey, E. J. W.; Overbeek, J. T. G. *Theory of the Stability of Lyophobic Colloids*; Elsevier: New York, 1948.
(36) Lide, D. R., Ed.; *Handbook of Chemistry and Physics*; CRC Press: Boca Raton, FL, 2004.
(37) Strikwerda, J. C. *Finite Difference Schemes and Partial Differential Equations*, 2nd ed.; SIAM Society for Industrial and Applied Mathematics: Philadelphia, 2004.
(38) Hildebrand, J. H.; Prausnitz, J. M.; Scott, R. L. *Regular and Related Solutions*; Van Nostrand Reinhold: New York, 1970.
(39) Nagarajan, R. Theory of Micelle Formation. In *Structure−Performance Relationships in Surfactants*, 2nd ed.;Esumi, K., Ueno, M., Eds.; Surfactant Science Series; Marcel Dekker: New York, 2003; Vol. *112*, Chapter 1.
(40) Perry, R. H., Green, D. W., Maloney, J. O., Eds. *Perry's Chemical Engineers' Handbook*, 7th ed.; McGraw-Hill: New York, 1997.
(41) Finney, J. L. *Proc. R. Soc. London, Ser. A* **1970**, *319*, 479−493.
(42) Carnahan, N. F.; Starling, K. E. *J. Chem. Phys.* **1969**, *51*, 635−636.
(43) Agterof, W. G. M.; van Zomeren, J. A. J.; Vrij, A. *Chem. Phys. Lett.* **1976**, *43*, 363−367.
(44) Overbeek, J. T. G. *Faraday Discuss. Chem. Soc.* **1978**, *65*, 7−19.
(45) Poling, B. E.; Prausnitz, J. M.; Connell, J. O. *The Properties of Gases and Liquids*, 5th ed.; McGraw-Hill: New York, 2000.
(46) Sørensen, J. M., Arlt, W., Eds.; *Liquid-Liquid Equilibrium Data Collection. 1, Binary Systems: Tables, Diagrams and Model Parameters*; DECHEMA: Frankfurt/Main, Germany, 1979; Vol. *5*.
(47) Viades-Trejo, J.; Amigo, A.; Gracia-Fadrique, J. *Fluid Phase Equilib.* **2006**, *250*, 158−164.
(48) Zheng, O.; Zhao, J.-X.; Fu, X.-M. *Acta Phys. Chim. Sin.* **2006**, *22*, 322−325.
(49) Bai, G.; Wang, J.; Yan, H.; Li, Z.; Thomas, R. K. *J. Phys. Chem. B* **2001**, *105*, 9576−9580.
(50) Zana, R. *J. Colloid Interface Sci.* **1980**, *78*, 330−337.
(51) Treiner, C.; Makayssi, A. *Langmuir* **1992**, *8*, 794−800.
(52) Caria, A.; Regev, O.; Khan, A. *J. Colloid Interface Sci.* **1998**, *200*, 19−30.
(53) Matsumoto, T. *Colloid Polym. Sci.* **1992**, *270*, 492−497.
(54) Kennedy, J.; Eberhart, R. *Proc. IEEE Int. Conf. Neural Networks* **1995**, *4*, 1943−1948.
(55) Schwaaba, M. Jr.; Biscaia, E. C.; Monteiro, J. L.; Pinto, J. C. *Chem. Eng. Sci.* **2008**, *63*, 1542−1552.
(56) Zhou, J. L.; Tits, A. L.; Lawrence, C. T. *User's Guide for FFSQP Version 3.7: A FORTRAN Code for Solving Constrained Nonlinear (Minimax) Optimization Problems, Generating Iterates Satisfying All Inequality and Linear Constraints*. University of Maryland: College Park, MD, 1997.
(57) Eriksson, J. C.; Ljunggren, S. *Langmuir* **1996**, *11*, 1145−1153.
(58) Sicoli, F.; Langevin, D. *J. Phys. Chem.* **1995**, *99*, 14819−14823.
(59) Georgii, H.-O. *Gibbs Measures and Phase Transitions*; De Gruyter Studies in Mathematics; W. de Gruyter: New York, 1988; Vol. *9*.